ORIGINAL ARTICLE

PM Cattaneo
M Dalstra
B Melsen

Strains in periodontal ligament and alveolar bone associated with orthodontic tooth movement analyzed by finite element

Authors' affiliation:
P.M. Cattaneo, M. Dalstra, B. Melsen,
Department of Orthodontics, School of Dentistry, University of Aarhus, Aarhus C, Denmark

Correspondence to:
Paolo M. Cattaneo
Department of Orthodontics
School of Dentistry
University of Aarhus
Vennelyst Boulevard 9
DK-8000, Aarhus C
Denmark
E-mail: pcattaneo@odont.au.dk

Dates:
Accepted 4 February 2009

To cite this article:
Cattaneo PM, Dalstra M, Melsen B:
Strains in periodontal ligament and alveolar bone associated with orthodontic tooth movement analyzed by finite element
Orthod Craniofac Res 2009;**12**:120–128

Structured Abstract

Authors – Cattaneo PM, Dalstra M, Melsen B

Introduction – Orthodontic tooth movement (OTM) is achieved by applying an orthodontic force system to the brackets. The (re)modeling processes of the alveolar support structures are triggered by alterations in the stress/strain distribution in the periodontium. According to the classical OTM theories, symmetric zones of compression and tension are present in the periodontium, but these do not consider the complex mechanical properties of the PDL, the alveolar structures' morphology, and the magnitude of the force applied.

Materials and Methods – Human jaws segments obtained from autopsy were microCT-scanned and sample-specific finite element (FE) models were generated. The material behavior of the PDL was considered to be nonlinear and non-symmetric and the alveolar bone was modeled according to its actual morphology. A series of FE-analyzes investigated the influence of the moment-to-force ratio, force magnitude, and chewing forces on the stress/strain in the alveolar support structures and OTM.

Results – Stress/strain findings were dependent on alveolar bone's morphology. Because of the nonlinear behavior of the PDL, distinct areas of tension, and compression could not be detected. Secondary load transfer mechanisms were activated and the stress/strain distribution in the periodontium was concealed by occlusal forces.

Conclusions – We could not confirm the classical ideas of distinct and symmetrical compressive and tensile areas in the periodontium in relation to different OTM scenarios. Light continuous orthodontics forces will be perceived as intermittent by the periodontium. Because roots and alveolar bone morphology are patient-specific, FE-analysis of orthodontic loading regime should not be based on general models.

Key words: finite element analysis; orthodontics; periodontal ligament; tooth movement

Introduction

Orthodontic tooth movement (OTM) occurs as a result of site-specific resorption and formation of the alveolar bone. The remodeling processes of the alveolar support structures are triggered by alterations in the stress/strain distribution in the periodontium caused by the intra-alveolar displacement of the roots within the intra-alveolar space. The amount and type of displacement is determined by the loading regime as well as by force magnitude. The displacement of the roots causes a cascade whereby a mechanical stimulus is turned into a biologic reaction, so that OTM becomes possible. This process, called *mechanotransduction,* involves bone modeling secondary to loading and is comprised *mechanocoupling, biomechanical coupling, cell-to-cell signaling,* and *effectors response* (1). The similarities between orthodontics and orthopedics seem therefore to be straightforward, but the presence of the periodontal ligament (PDL) makes a direct application of orthopedic concepts to orthodontics more complex. The PDL being a nonlinear, multi-phasic, and visco-elastic material (2–4) substantially influences the load transfer from the teeth to the surrounding alveolar bone.

A common goal for all orthodontists has been to define a force that results in a maximal rate of tooth movement with minimal iatrogenic side-effects. A thorough knowledge of the loading of the different tissues involved in OTM is needed as the basis for improved understanding of the *mechanotransduction*. Two main theories regarding tissue reaction to orthodontic loading have been proposed: the 'pressure–tension' theory (5, 6), and the distortion or bending of the alveolar bone also referred as 'bioelectric' theory (7–10). Lately, the cellular reaction of the alveolar bone has been perceived as a reflection of the local state of loading (11). A way to verify the validity of the theories mentioned above and to investigate the effects of orthodontic loading regimes would be to determine point by point the stress and strain distributions within the whole periodontium following the application of orthodontic forces. The finite element method (FEM) has proved to be a valid and reliable technique for the calculation of the local state of deformation and loading of complex structures. However, the validity of the results of FE-analyzes is totally dependent on the ability to model the complexity of morphology and tissues material properties of the structures analyzed (12, 13).

The aim of the present investigation was therefore to use the FEM: 1) to describe the orthodontic load transfer from the teeth to the alveolus; 2) to determine the influence of force magnitude in the stress and strain distribution in the alveolar support structures; and 3) to study the interactions of occlusal and orthodontic forces.

Materials and methods

A simplified FE-model of a tooth from an experiment described previously (14) was used to evaluate the shape of the tooth socket wall when a translation movement was simulated. Subsequently, two humans segments from two different donors were harvested at autopsy (approval obtained from Aarhus University Ethical Committee). The first specimen was a frontal left segment of a mandible and the second was a posterior left segment of the mandible. Using a microCT (μCT) scanner (μCT40; Scanco Medical, Bassersdorf, Switzerland) two three-dimensional (3D) datasets of the segments were generated (Fig. 1). Using a procedure described previously (12), 3D FE-models were generated comprised alveolar bone, PDL, and for the first sample, canine and first premolar (Fig. 2, left), and for the second sample, first and second molars (Fig. 2, right).

Material properties

The material properties of the elements representing alveolar bone were assigned using a procedure where the Young's modulus of each element was allocated individually based on the information retrieved from the μCT-scans so that the bone structure, including trabecular structures, could be modeled on a tissue level (15). Three different Young's moduli were chosen to represent full cortical bone (17 500 MPa, Poisson's ratio of 0.3), partly cortical bone (5000 MPa, Poisson's ratio of 0.3), and bone marrow (200 MPa, Poisson's ratio of 0.3). A nonlinear and non-symmetric approach was used to describe the material properties of the PDL, and a Poisson's ratio of 0.3 was used (3, 12, 16–18). The elements representing the teeth were assigned a Young's modulus of 20 000 MPa and a Poisson's ratio of 0.3 (19–21).

Loading and boundary conditions

In the simplified model, the force magnitude was set at 100 cN and a pure translation movement was

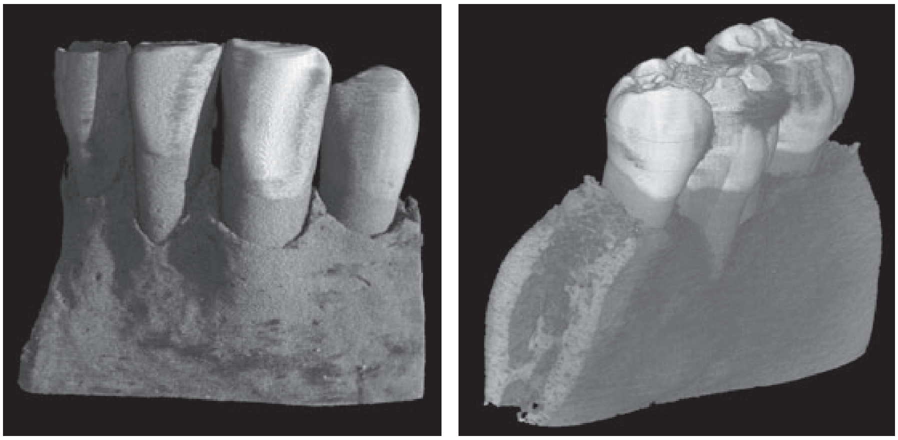

Fig. 1. Rendering of the 3D μCT dataset of the left anterior segment of the mandible with the incisors, premolar, and canine (left) and rendering of the 3D μCT dataset of the left posterior segment of the mandible with the second premolar, first and second molar (right). Voxel dimension is 37 μm.

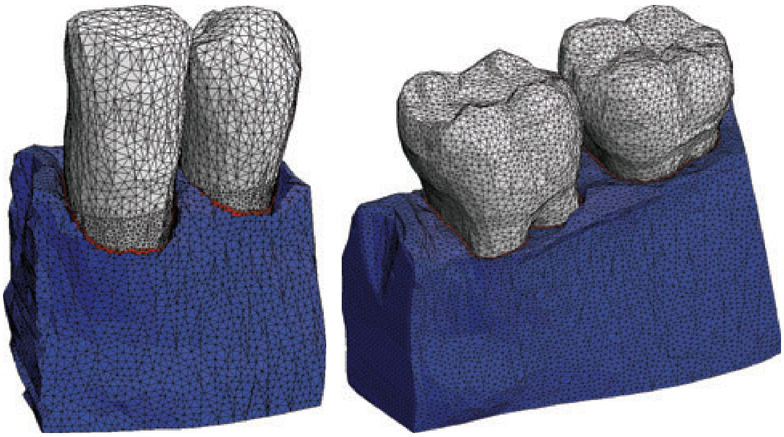

Fig. 2. FE-models of the human segments presented in Fig. 1. Note that only a portion of the samples were used to generate the FE-models.

***Table 1.* Summary of the various orthodontic loading regimes for the teeth, used in the experiments**

Load case	M/F @ canine	M/F @ premolar	M/F @ 1st molar	M/F @ 2nd molar	Force magnitude [cN]
I	0	0	0	0	100*
	11	9	11	12	
II	0	0	0	–	0–400*
III	–	–	0	–	100* & 0–20 000†

*Orthodontic forces.
†Occlusal forces.

achieved by constraining root movement to the mesial-distal direction. For the human-based FE-models, a range of orthodontic loading regimes were simulated in accordance with clinical practice. In the first series of analyzes, the effects of a force of 100 cN acting on a bucco-lingual direction and two different moment-to-force (M/F) ratio were analyzed (Table 1). The force was acting in a buccal direction on the premolar and second molar, and lingually on the canine and first molar. The M/F ratio for the canine, first and second molar was chosen to be either 0 or 11, whilst for the premolar 0 or 9 (22). In the second series of analyzes, the influence of force magnitude on the load transfer mechanism was evaluated. A fixed M/F ratio of zero was used for the first premolar, the canine, and first molar, whereas the force magnitude was progressively increased up to 400 cN in steps of 50 cN. In the third series of analyzes, occlusal vertical forces ranging from 0 to 20 000 cN were superimposed to an orthodontic force of 100 cN and a M/F of 0. For each series of analyzes the stress and strain distribution in the periodontium, and the resulting tooth movements were ascertained. Movement was suppressed in all directions for the nodes situated on the bottom edge of each bone segments.

Results

Simplified FE-model

The FE-analysis showed that the deformation of the alveolar wall in a buccal–lingual cross-section occurred mostly on the tension side (Fig. 3B, C, upper-right quadrant). The concavity of the alveolar wall was decreasing at X (the area where bone apposition occurs) but it is increasing at Y. When bending of the alveolar bone in a buccal–lingual section was assessed, the deformation at the cervical level was below 1 μstrain in case of tipping (Fig. 3, lower-left quadrant) and was approximately 0.1 μ strain in case of translation (Fig. 3, lower-right quadrant).

Sample-specific FE-models – orthodontic loading

1) When a M/F = 0 was simulated and the force level kept at 100 cN, all the teeth displayed uncontrolled tipping. Regions of compressive and tensile normal stresses could be identified in the PDL. However, the magnitude of the tensile stresses was significantly higher than the compressive stresses. This was consistent for all the teeth (Fig. 4). The accompanying strains in the PDL were in the range of −20% to 14%. The distinct compression and tension areas seen in the PDL were not present in the adjacent areas of the alveolar bone, except for a thin layer of bone in close contact with the PDL. Areas of tensile stress were well recognizable in the lingual-cervical and buccal-apical alveolar bone. In the bucco-cervical area of the alveolar bone the compressive stresses are barely detectable. The same is seen on the lingual-apical portion of the alveolar bone (Fig. 5, upper row).

When M/F's of 9 and 11 at 100 cN were simulated, all teeth displayed almost perfect translation. As a consequence, the overall displacements of the teeth were smaller than in the case of uncontrolled tipping. In the lingual section of the PDL of the canine and first molar, and on the buccal section in case of the premolar, a nearly uniform distribution of tensile stresses were present, whereas a very mild compression was present on the opposed side of the PDL (Fig. 6). In the alveolar bone on the 'tension' side the tensile stresses were uniformly distributed with a maximum value of about 0.02 MPa (for the premolar), whilst on the opposite

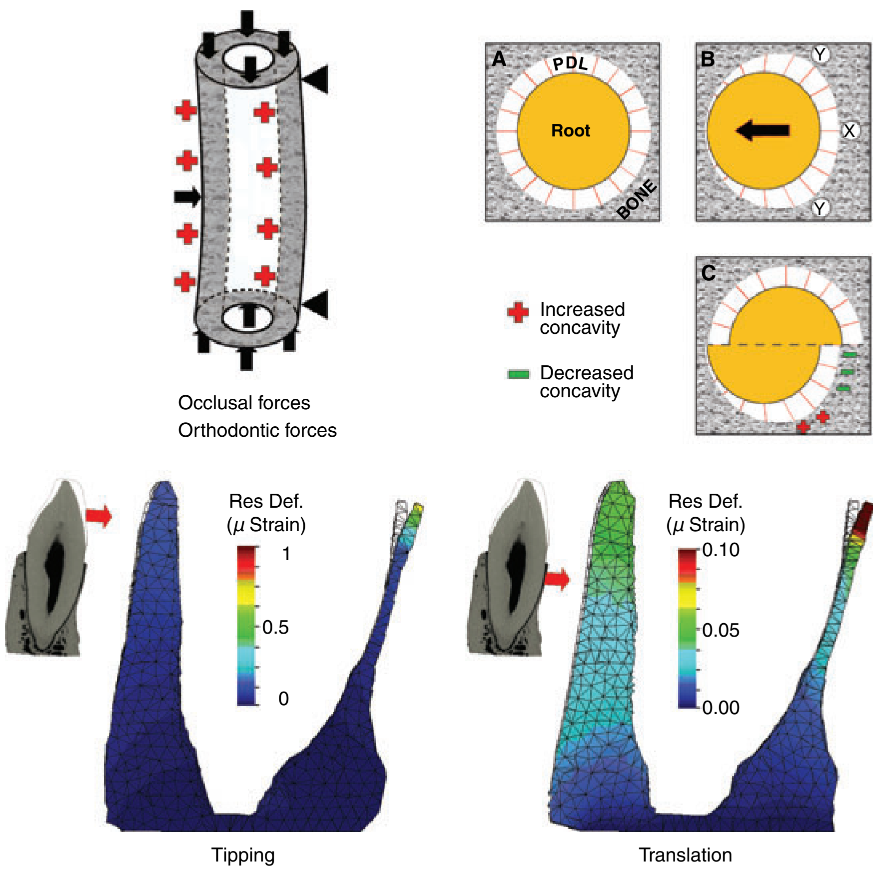

Fig. 3. Top-left: deformation of a long bone when longitudinal and lateral forces are applied. The arrows show the loading application and direction; the '+' signs indicate the increased concavity; C, compression side; T, tension side [adapted from Epker & Frost (24) & Meikle (28)]. Top-right: cross-section perpendicular to the long axis of a single-rooted tooth (A). Deformation of the alveolar wall and of the PDL fibers when an orthodontic force is applied (500× magnification) (B). A decrease of the concavity of the bony wall (−) is shown where there is apposition and increased concavity (+) on the lateral aspects of the alveolar wall (C). Bottom: deformation of the alveolar bone is depicted when simulating uncontrolled tipping (left; force = 100 cN, M/F = 0), and translation (right; force = 100 cN, M/F = 11). The deformed shape is depicted using a color-code, whilst for the non-deformed section, white is used (100× magnification). A μCT-reconstructed slice representing the same section is depicted for clarity.

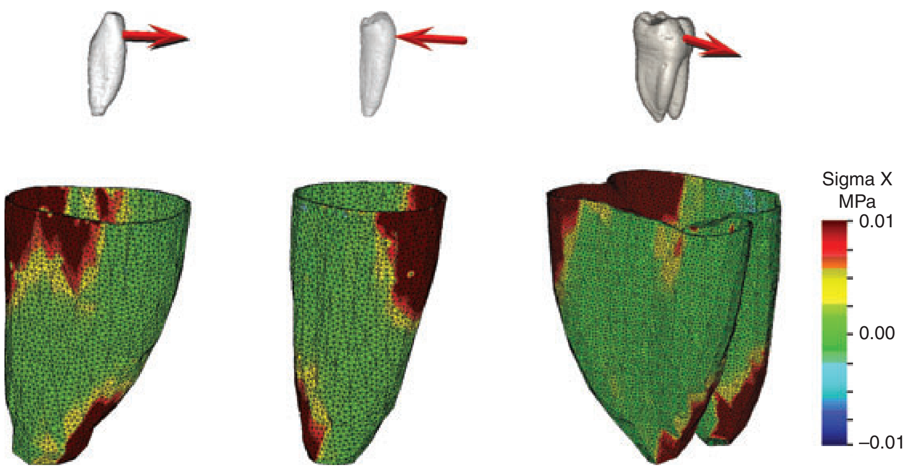

Fig. 4. Stress along the buccal–lingual direction, σ_x, at the bone–PDL interface around the root of the canine (left), the premolar (center), and the first molar (right). The negative values represent compression whilst the positive tension. The force level was kept constant at 100 cN during the analyzes and a M/F ratio of 0 was used (i.e. uncontrolled tipping).

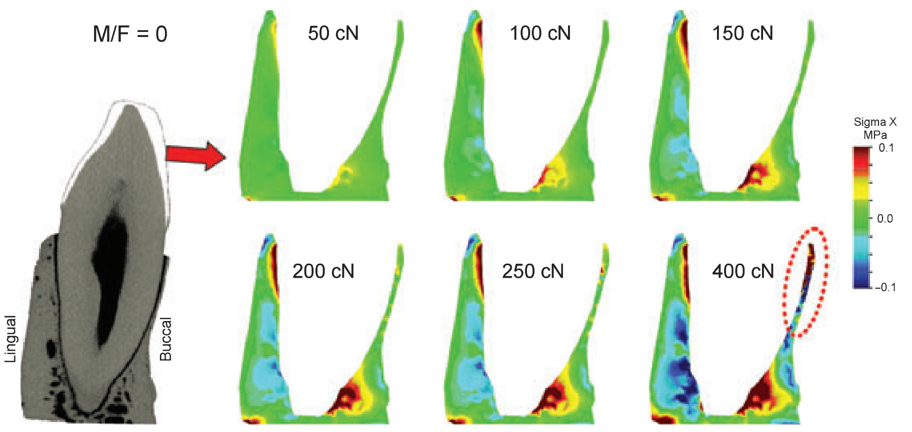

Fig. 5. Lingual-buccal stress, σ_x, in a transversal section of the alveolar bone passing through the long axis of the canine when the force level is varied from 0 to 400 cN and the M/F ratio is set to 0. The negative values represent compression whilst the positive tension. Note that bone in the buccal cervical region is loaded only when the applied orthodontic force becomes larger than 200 cN. A μCT-reconstructed slice representing the same section is depicted for clarity.

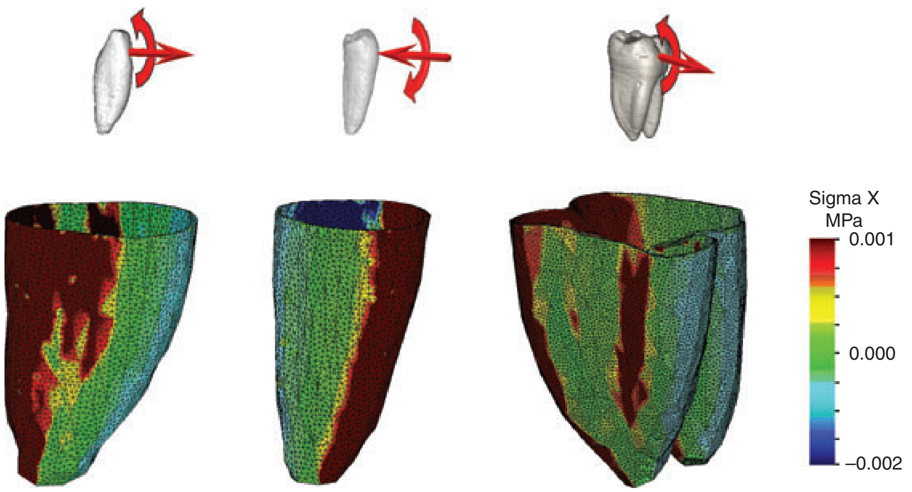

Fig. 6. Stress along the buccal–lingual direction, σ_x, at the bone–PDL interface around the root of the canine (left), the premolar (center), and the first molar (right). The negative values represent compression whilst the positive tension. The force level was kept constant at 100 cN during the analyzes and a M/F ratio of 11 was used for the canine and first molar and of 9 for the premolar (i.e. translation).

side the compressive stresses were by far lower with a maximum value of about 0.001 MPa (for the canine).

2) In the second series of experiments, the force level was gradually increased. When the force magnitude was below 150 cN, the state of stress/strain and deformation in the PDL was mimicking what had been found in the first series of analyzes. In contrast, when force magnitude became larger than 200 cN, a small area of compression started to appear in the PDL at the level of the crest of alveolar bone and in the direction of the force. At a level of 400 cN, the peak value of compressive stresses was similar to what was found on the tensile side, nevertheless, the area did not substantially increased in size (Fig. 7). At a force level of 400 cN the PDL in the

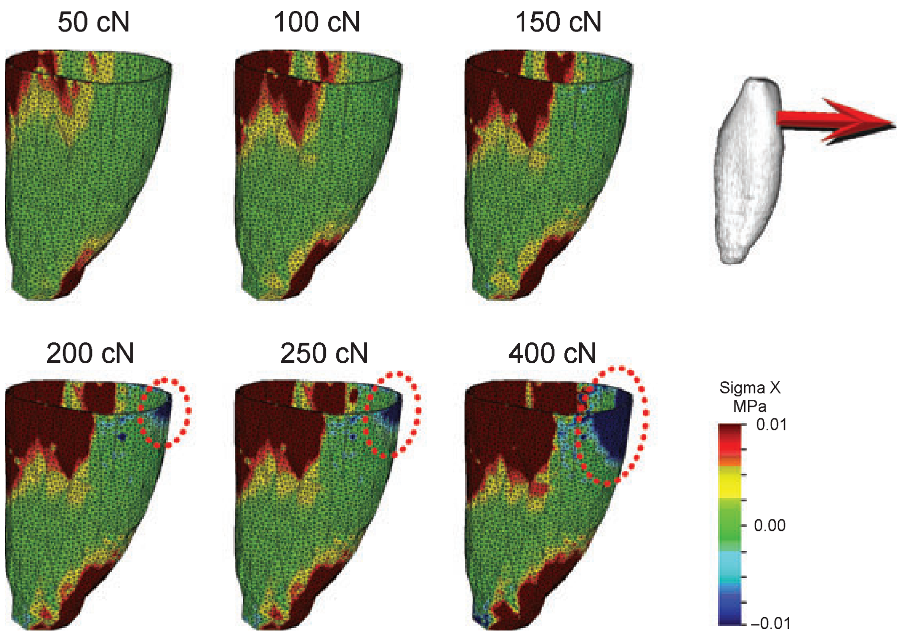

Fig. 7. Stress along the buccal–lingual direction, σ_x, at the bone–PDL interface around the root of the canine. The negative values represent compression whilst the positive tension. The M/F ratio was kept constant at 0 during the analyzes while the force was increased up to 400 cN. Note that areas where high compressive stresses are detected (circles) start to appear when forces become larger than 200 cN.

buccal- and lingual-cervical level has been deformed more than 80%. The area where compressive stresses were present was immediately bordered by areas where no compression could be detected. The compressive stresses in the PDL were transferred to the adjacent alveolar bone, where they were transformed into compressive as well as tensile hoop stresses, as demonstrated in a previous research (12) (Fig. 5, lower row).

Sample-specific FE-models – orthodontic and occlusal loading

In the last series of analyzes, the influence of the occlusal forces on the stress and strain distribution in the PDL was investigated. When the vertical-occlusive force reached a magnitude up to approximately 500 cN, no substantial changes could be detected in the PDL from the scenario where only the orthodontic loading forces were applied. Beyond this level, the loading of the PDL and of the alveolar structures in general became completely different, changing from uncontrolled tipping (because of the orthodontic forces) to pure intrusive movement (because of occlusal forces; Fig. 8).

Discussion

Changes in the stress and strain distribution are the triggers for bone modeling that allow the teeth to move when an orthodontic loading regime is applied at the bracket. The present investigation describes how the loading pattern influences the first steps of the *mechanotransduction* mechanism leading to PDL re-arrangement and bone resorption and formation in relation to OTM. These findings do not corroborate the simplified view of having tensile and compressive stresses in separate areas of the PDL and alveolar bone (12, 23, 24), which characterized the classical '*pressure–tension*' theory (5, 6). Bone formation related to an increased concavity of the alveolar bone wall also could not be confirmed (8). Moreover, the change in curvature of the alveolar socket could not be compared with long bones (9, 24). What is presented in this study corroborates what was previously speculated (11): bone formation is the result of an increase state of load in the alveolar bone and in the stretched PDL fibers, while bone resorption is the results of either an unload state (i.e. *direct resorption*) or as a consequence of hyalinization (i.e. *indirect* or *undermining resorption*) in the area where the PDL is undergoing large compressive deformation and the underlying alveolar bone is subjected to local high stress and strain (25).

Since the pioneering research on tooth movement performed by Sandstedt (26), hyalinization has been described as an almost unavoidable phenomenon associated with orthodontics movement (27). Though hyalinization takes place even when light orthodontic forces are used, hyalinization areas are more likely to

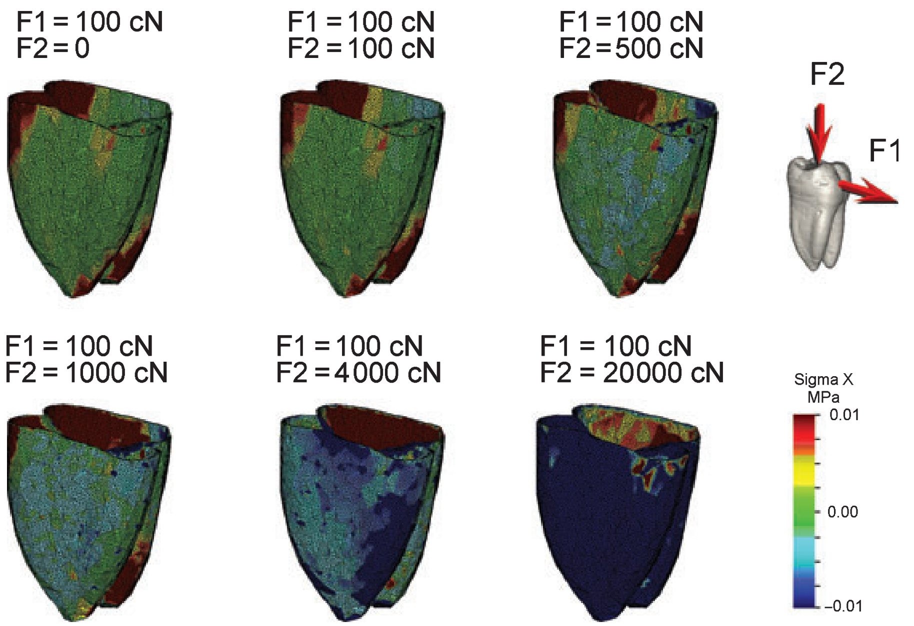

Fig. 8. Stress along the buccal–lingual direction, σ_x, at the bone–PDL interface around the root of the first molar. The negative values represent compression whilst the positive tension. The orthodontic loading regime was kept constant (F1 = 100 cN and M/F = 0) while the vertical occlusal force (F2) was increased up to 200 N. Note that the stress distribution substantially changes for F2 > 500 cN.

occur when high forces are used, and more in cases of tipping than in bodily movement (6, 27, 28). Dalstra et al. (29) showed that the alveolar bone surface is not smooth and therefore even small orthodontic loading can give rise to local high stress and strain. In order to minimize hyalinization areas and thus increasing tooth movement rate, the search for an optimal force magnitude has been investigated (30, 31), even though some authors have been skeptical about this concept (32, 33) and data in the literature are not exhaustive (34). On the other hand, Ren et al. (33) stated that 'a dose–response relationship exists in the very low force range; then a plateau is reached'.

The present study showed that small forces were enough to produce deformations in the PDL, yet the associated compressive stresses were very mild. However, by increasing force magnitude during uncontrolled tipping the compressive stresses in the PDL increased considerably and compressive forces were transferred to the cervical portion of the alveolar bone. This would give rise to local ischemia in the PDL, followed by the formation of a hyalinised area, leading to local necrosis of the underlying alveolar bone. Before the tooth can further move, the necrotic bone has to be removed by *undermining resorption*. This might explain while at low forces a dose–response relationship exists, whilst by further increasing the forces magnitude will not lead to an increased tooth movement rate (33). On the other hand, areas characterized by high compressive stresses are limited and they are directly bordered by areas with a state of no- or low-compression, where it is anticipated that direct (frontal) resorption is taking place.

The morphology and material properties of the tissues forming the periodontium are characterized by a high level of complexity. When mathematical models are used to mimic these structures, it is understood that some simplifications have to be introduced; however, these should not be detrimental to the correctness of the results. In the present study, an approximation of the true physical properties of PDL was used, where its basic shape with a low-stiffness toe region and a high-stiffness slope closely resembled both experimentally (3) and mathematically determined relationships (35). Datasets from μCT allowed precise descriptions of both the external geometry and the internal morphology of the alveolar bone. The force magnitude of 100 cN and the occlusal force magnitudes were chosen based on good accordance with the magnitude of forces used in clinical practice (4, 10, 36, 37). In this study, translation was best approximated by using a M/F ratios of 11 for the canine, the first and second molar, and 9 for the premolar (22), values that differ somewhat from those previously proposed by Burstone and Pryputniewicz (37). A limitation of the present study is that the results could not be directly compared with *in vivo* loading; nevertheless, the calculated amount of deflection of the teeth reflects what has been reported in experimental studies (4, 38). Nevertheless, a fine tuning of the FE-models and of the material properties of the various tissues is necessary in order to better determine the stress and strain distributions within the whole periodontium and the transition between low and high forces under orthodontic loading.

Conclusions

The present FE-analyzes indicate that following the application of an orthodontics loading regime, alveolar bone modeling cannot be based on the simplified, yet generally accepted, concept of resorption caused by compression, and formation caused by tension.

Clinical relevance

With OTM, there is an on-going tendency toward the use of lighter forces in order to approximate an optimal force resulting in a maximal rate of OTM with minimal iatrogenic side-effects. This study provides insights into the stress and strain distribution, calling into question the classic idea of symmetric compressive, and tensile areas. Our investigations suggest that a more thorough knowledge of the state of loading of the different tissues involved in OTM may be useful for determining force levels to be used clinically, minimizing hyalinization, and thus defining the ideal range for orthodontics forces.

References

1. Turner CH, Pavalko FM. Mechanotransduction and functional response of the skeleton to physical stress: the mechanisms and mechanics of bone adaptation. *J Orthop Sci* 1998;3:346–55.
2. Wills DJ, Picton DC, Davies WI. A study of the fluid systems of the periodontium in macaque monkeys. *Arch Oral Biol* 1976;21:175–85.
3. Toms SR, Lemons JE, Bartolucci AA, Eberhardt AW. Nonlinear stress-strain behavior of periodontal ligament under orthodontic loading. *Am J Orthod Dentofacial Orthop* 2002;122:174–9.
4. Christiansen RL, Burstone CJ. Centers of rotation within the periodontal space. *Am J Orthod Dentofacial Orthop* 1969;55:353–69.
5. Schwartz AM. Tissue changes incidental to orthodontic tooth movement. *Int J Orhodontia* 1932;18:331–52.
6. Reitan K. The initial tissue reaction incident to orthodontic tooth movement as related to the influence of function. *Acta Odontol Scand* 1951;6:1–240.
7. Baumrind S. A reconsideration of the propriety of the ''pressure–tension'' hypothesis. *Am J Orthod Dentofacial Orthop* 1969;55:12–22.
8. Heller IJ, Nanda R. Effect of metabolic alteration of periodontal fibers on orthodontic tooth movement. An experimental study. *Am J Orthod Dentofacial Orthop* 1979;75:239–58.
9. Frost HM. Wolff's Law and bone's structural adaptations to mechanical usage: an overview for clinicians. *Angle Orthod* 1994;64:175–88.
10. Proffit WR, Fields HW, Sarver DM. *The Biological Basis of Orthodontic Therapy. Contemporary Orthodontics*. St Louis, MO: Mosby, Elsevier; 2007. pp. 329–58.
11. Melsen B. Tissue reaction to orthodontic tooth movement – a new paradigm. *Eur J Orthod* 2001;23:671–81.
12. Cattaneo PM, Dalstra M, Melsen B. The finite element method: a tool to study orthodontic tooth movement. *J Dent Res* 2005;84:428–33.
13. Viecilli RF, Katona TR, Chen J, Hartsfield JK Jr, Roberts WE. Three-dimensional mechanical environment of orthodontic tooth movement and root resorption. *Am J Orthod Dentofacial Orthop* 2008;133:791.e11–791.e26.
14. Melsen B, Dalstra M, Cattaneo PM. Reaction Osseuse au Deplacement Dentaire Provoque/Osseus reaction to orthodontic tooth movement. *J Paradontolog d'Implantolog Orale* 2001;20:313–29.
15. Cattaneo PM, Dalstra M, Frich LH. A three-dimensional finite element model from computed tomography data: a semi-automated method. *Proc Inst Mech Eng [H]* 2001;215:203–13.
16. Nishihira M, Yamamoto K, Sato Y, Ishikawa H, Natali AN. Mechanics of periodontal ligament. In: Natali AN, editor. *Dental Biomechanics*. London: Taylor & Francis CRC Press; 2003. pp. 20–34.
17. Poppe M, Bourauel C, Jager A. Determination of the elasticity parameters of the human periodontal ligament and the location of the center of resistance of single-rooted teeth. A study of autopsy specimens and their conversion into finite element models. *J Orofac Orthop* 2002;63:358–70.
18. Vollmer D, Bourauel C, Maier K, Jager A. Determination of the centre of resistance in an upper human canine and idealized tooth model. *Eur J Orthod* 1999;21:633–48.
19. Verdonschot N, Fennis WM, Kuijs RH, Stolk J, Kreulen CM, Creugers NH. Generation of 3-D finite element models of restored human teeth using micro-CT techniques. *Int J Prosthodont* 2001;14:310–5.
20. Bourauel C, Freudenreich D, Vollmer D, Kobe D, Drescher D, Jager A. Simulation of orthodontic tooth movements. A comparison of numerical models. *J Orofac Orthop* 1999;60:136–51.
21. Tanne K, Sakuda M, Burstone CJ. Three-dimensional finite-element analysis for stress in the periodontal tissue by orthodontic forces. *Am J Orthod Dentofacial Orthop* 1987;92:499–505.
22. Cattaneo PM, Dalstra M, Melsen B. Moment-to-force ratio, center of rotation, and force level: a finite element study predicting their interdependency for simulated orthodontic loading regimens. *Am J Orthod Dentofacial Orthop* 2008;133:681–9.
23. Cattaneo PM, Dalstra M, Melsen B. Load transfer around orthodontically moved teeth by means of finite element analysis. In: Davidovitch M, Mah J, Suthanarak S, editors. *Biological Mechanism of Tooth Eruption, Resorption and Movement*. Boston, MA: Harward Society for the Advancement of Orthodontics; 2006. pp. 253–60.

24. Epker BN, Frost HM. Correlation of bone resorption and formation with the physical behavior of loaded bone. *J Dent Res* 1965;44:33–41.
25. Thilander B, Rygh P, Reitan K. Tissue reactions in orthodontics. In: Vanarsdall, Jr., RL, Vig, KWL, editors. *Orthodontics – Current Principles & Techniques*. St Louis, MO: Elsevier-Mosby; 2005. pp. 145–219.
26. Persson M. A 100th anniversary: Sandstedt's experiments on tissue changes during tooth movement. *J Orthod* 2005;32:27–8.
27. Reitan K. Clinical and histologic observations on tooth movement during and after orthodontic treatment. *Am J Orthod* 1967;53:721–45.
28. Meikle MC. The tissue, cellular, and molecular regulation of orthodontic tooth movement: 100 years after Carl Sandstedt. *Eur J Orthod* 2006;28:221–40.
29. Dalstra M, Cattaneo PM, Beckmann F. Synchrotron radiation-based microtomography of alveolar support tissues. *Orthod Craniofac Res* 2006;9:199–205.
30. Storey E, Smith R. Force in orthodontics and its relation to tooth movement. *Aust J Dent* 1952;56:11–8.
31. Choy K, Pae EK, Park Y, Kim KH, Burstone CJ. Effect of root and bone morphology on the stress distribution in the periodontal ligament. *Am J Orthod Dentofacial Orthop* 2000;117:98–105.
32. Pilon JJGM, KuijpersJagtman AM, Maltha JC. Magnitude of orthodontic forces and rate of bodily tooth movement. An experimental study. *Am J Orthod Dentofacial Orthop* 1996;110:16–23.
33. Ren Y, Maltha JC, 't Hof MA, Kuijpers-Jagtman AM. Optimum force magnitude for orthodontic tooth movement: a mathematic model. *Am J Orthod Dentofacial Orthop* 2004;125:71–7.
34. Ren Y, Maltha JC, Kuijpers-Jagtman AM. Optimum force magnitude for orthodontic tooth movement: a systematic literature review. *Angle Orthod* 2003;73:86–92.
35. Pietrzak G, Curnier A, Botsis J, Scherrer S, Wiskott A, Belser U. A nonlinear elastic model of the periodontal ligament and its numerical calibration for the study of tooth mobility. *Comput Methods Biomech Biomed Engin* 2002;5:91–100.
36. Burstone CJ. The biomechanics of tooth movement. In: Kraus BS, Ripamonti A, editors. *Vistas in Orthodontics*. Philadelphia, PA: Lea and Febinger; 1962. pp. 197–213.
37. Burstone CJ, Pryputniewicz R-J. Holographic determination of centers of rotation produced by orthodontic forces. *Am J Orthod Dentofacial Orthop* 1980;77:396–409.
38. Jones ML, Hickman J, Middleton J, Knox J, Volp C. A validated finite element method study of orthodontic tooth movement in the human subject. *J Orthod* 2001;28:29–38.